

Role of Precursor Molecular Structure on the Microstructure and High Temperature Stability of Silicon Oxycarbide Glasses Derived from Methylene-Bridged Polycarbosilanes

Gian Domenico Sorarù

Università di Trento, Dipartimento di Ingegneria dei Materiali, Via Mesiano 77,
38100, Trento, Italy

Q. Liu, Leonard V. Interrante,* and T. Apple

Department of Chemistry Rensselaer Polytechnic Institute, Troy, New York 12180

Received July 6, 1998. Revised Manuscript Received October 9, 1998

Cross-linked polycarbosilane/siloxane hybrid polymers were synthesized by sol-gel processing of both the linear and the hyperbranched alkoxy-substituted polycarbosilanes of the type $[\text{Si}(\text{OR})_2\text{CH}_2]_n$, where R = Me or Et. The molecular structure of these gels and their pyrolysis to silicon oxycarbide ceramics were investigated by elemental analysis, thermogravimetric analysis, FT-IR, and solid-state (SS)NMR spectroscopies. The microstructure of the polymer gels and their pyrolysis products were investigated by nitrogen adsorption-desorption experiments (the BET test). SSNMR and IR spectra show that the initial gels after drying have a complex structure involving siloxy linkages and pendant Si-OR (R = H, Me or Et) groups in addition to the initial Si-CH₂-Si bonding in the starting carbosilanes. After heating to 600 °C, the gels become nearly fully condensed with an approximate $[\text{Si}(\text{O})\text{CH}_2]_n$ average formula, except in the case of the gel derived from the hyperbranched $[\text{Si}(\text{OMe})_2\text{CH}_2]_n$ polycarbosilane, which still contains appreciable Si-OH groups. Between ca. 600 and 1000 °C, conversion to an inorganic structure occurs, which is accompanied by extensive redistribution reactions involving the exchange of Si-O and Si-C bonds. Particularly in the case of the $[\text{Si}(\text{OMe})_2\text{CH}_2]_n$ -derived gel, this is likely facilitated by a Si-OH-induced attack on the Si-CH₂-Si linkages, leading to additional siloxy linkages and terminal Si-CH₃ bonds. All of the investigated gels and their pyrolysis products were found to have relatively high surface areas and a microporous structure. Moreover, the results of this work indicate that the molecular structure of the starting carbosilane, as well as the degree of hydrolysis and condensation in the initial gel, has an significant effect on both the pyrolysis chemistry of the gel and the composition and the microstructure of the ceramic product which, in turn, strongly affects its high-temperature stability.

Introduction

In the last 2 decades powder-free chemical methods for the preparation of advanced ceramics have been developed as an alternative to the classical powder processing routes. Non-oxide ceramics (SiC, Si₃N₄ and even multicomponent Si-C-N-B-based materials) have been obtained by pyrolysis of certain preceramic polymers¹ while oxide glasses and ceramics have been produced by the sol-gel method.² Silicon oxycarbide can be viewed as a hybrid of the non-oxide (SiC) and oxide (SiO₂) systems, both from a structural perspective and in terms of its properties. Indeed, the substitution of tetravalent carbon atoms for the divalent oxygens in the silica network leads to an increase of the connectivity

with a corresponding improvement of many physical, chemical, and thermal properties.³ Accordingly, SiO_xC_y glasses have been proposed for a number of different applications, including matrixes for ceramic matrix composites (CMCs)^{4,5} and porous catalyst supports.⁶

Currently, the most promising processing routes for the production of SiO_xC_y glasses involve the pyrolysis in an inert atmosphere of hybrid organic/inorganic networks obtained either by cross-linking of siloxane polymers⁷ or by sol-gel reactions of modified silicon

(1) *Materials Science and Technology, A Comprehensive Treatment, Vol. 17B, Processing of Ceramics Part II*; Brook, R. J., Ed.; VCH: Wurzburg, 1996; p 1.

(2) Brinker, C. J.; Scherrer, G. W. *Sol-Gel Science*; Academic Press: New York, 1990.

(3) Renlund, G. M.; Prochazka, S.; Doremus, R. H. *J. Mater. Res.* **1991**, *6*, 2723.

(4) Hurwitz, F. I.; Heimann, P. J.; Gyekenyesi, J. Z.; Masnovi, J.; Bu, X. Y. *Ceram. Eng. Sci. Proc.* **1991**, *12*, 1292.

(5) Carri, P.; Sorarù, G. D. Sol-Gel Processing of Continuous Fiber Reinforced Composites by the Liquid Infiltration and Pyrolysis (Lip) Method. *Innovative Processing and Synthesis of Ceramics, Glasses and Composites*; Bansal, N. P., Logan, K. V., Singh, J. P., Eds.; Ceramic Trans.: 1997; Vol. 85, p 405–416.

(6) Singh, A. K.; Pantano, C. G. *J. Am. Ceram. Soc.* **1996**, *79*, 2696.

(7) Renlund, G. M.; Prochazka, S.; Doremus, R. H. *J. Mater. Res.* **1991**, *6*, 2716.

alkoxides.⁸ In both cases the pyrolysis products consist of an amorphous silicon oxycarbide network, $\text{SiC}_x\text{O}_{2(1-x)}$, which contains carbidic (CSi_4) carbon units, along with a free carbon phase. It is worthy of note that the improvement of many silicon oxycarbide properties compared to the parent oxide system depends only (strictly) on the amount of carbon directly bonded to silicon in the $\text{SiC}_x\text{O}_{2(1-x)}$ network, since free carbon acts as an inert secondary phase.⁹ Moreover, it has been recently shown that the presence of free carbon can be detrimental for the high-temperature stability of SiO_xC_y glasses both in oxidizing¹⁰ and in reducing atmospheres.¹¹ For these reasons, the problem of controlling the composition of the amorphous oxycarbide network as well as the presence of free carbon has been addressed by several research groups. The amount of carbidic carbon seems inversely related to the O/Si atomic ratio of the starting preceramic network,^{12–15} while the free carbon phase can be reduced to almost zero if Si–H as well as Si–Me moieties are present in the starting siloxane network.^{16,17}

Despite the considerable information available regarding the relationship between the composition of the siloxane network and the composition of the resulting SiO_xC_y glass, little understanding of the possible influence of the precursor molecular structure on the ceramic microstructure has been developed. In this paper the microstructural evolution during pyrolysis of three polycarbosilane/siloxane materials having a similar chemical composition but different molecular structures has been followed through surface area and pore size distribution measurements. Also, the high-temperature stability of the SiO_xC_y glasses has been investigated by thermogravimetric analysis. It will be shown that the precursor architecture plays an important role in controlling the microstructure of the resulting silicon oxycarbide glass, which, in turn, strongly affects its high-temperature stability.

Experimental Procedure

Preparation of Gels from Alkoxy-Substituted Polycarbosilanes. The synthesis of the linear diethoxy polycarbosilane $[\text{Si}(\text{OEt})_2\text{CH}_2]_n$ (L-EPCS) has been described previously.¹⁸ The branched ethoxy-substituted polycarbosilane B-EPCS was synthesized by a modification of a previously published procedure.^{13,19–21} ¹H NMR (ppm): δ 0.2–1.0 (mul-

tiplets, SiCH_2Si and SiCH_3), 1.0–1.5 (OCH_2CH_3), 3.80 (OCH_2CH_3). ²⁹Si NMR (ppm): δ –46 ($\text{CH}_2\text{Si}(\text{OEt})_3$ (T units)), –20 (various $(\text{CH}_2)_2\text{Si}(\text{OEt})_2$ (D units)), 2 ($(\text{CH}_2)_3\text{Si}(\text{OEt})$ (M units)), –10 ($(\text{CH}_2)_4\text{Si}$ (C units)). ¹³C NMR (ppm): δ 20 (OCH_2CH_3), 60 (OCH_2CH_3), –4–10 (broad, SiCH_2Si)

The preparation of the dried gel from B-EPCS was carried out by following a similar procedure to that previously described for the L-EPCS system.¹⁸ The B-EPCS polymer (0.16 mol) was dissolved in ethanol (29 g, 0.63 mol, molar ratio to Si, 4:1) at ca. 50 °C. Then H_2O (11.35 g; 0.63 mol; molar ratio to Si, 4:1; in the form of a 1 M HCl aqueous solution) was introduced. The gelled solution was aged overnight at 50–60 °C. After stripping off the solvents under vacuum, the gel was dried under vacuum at ca. 60 °C for at least 6 h, yielding a coarse white powder.

The same procedure (including the same molar proportions of polycarbosilane, alcohol, and water) was followed to prepare the gel precursor from the hyperbranched methoxy-substituted polycarbosilane (B-MPCS), except that methanol was used in the preparation of the monomer for the polycarbosilane synthesis, i.e., chloromethyldimethoxychlorosilane, $\text{ClCH}_2\text{Si}(\text{MeO})_2\text{Cl}$, and as the solvent instead of ethanol in the sol-gel process for the resulting hyperbranched polycarbosilane.

Conversion of the Dried Gels into Silicon Oxycarbide Ceramics. The pyrolyses were conducted in a temperature-programmed CM high-temperature furnace by following a similar procedure to that employed in our previous studies.^{18,22} The gel was placed in a molybdenum or an alumina boat and was transferred to a gastight furnace tube. Nitrogen was used to flush out the air and protect the sample during the pyrolysis. The sample was flushed with N_2 for ca. 15 min before heating was started and then the sample was heated to 600 or 1000 °C at 5 °C/min under a continuous flow of N_2 , yielding a coarse, black powder. When the set temperature stage was reached, the furnace tube was taken out and cooled to room temperature by a fan while the sample was still under flowing N_2 . Samples at different temperatures were taken for elemental analysis, FTIR, and solid-state NMR analyses.

Measurements. The NMR spectra of the polymers were obtained with an Unity-300 instrument. ¹H and ¹³C spectra were referenced to the solvent (C_6D_6) peaks. ²⁹Si NMR spectra of the polymers were obtained in C_6D_6 solution with 0.1% (wt) of $\text{Cr}(\text{acac})_3$ as relaxation agent (90° pulse, 20 s delay).

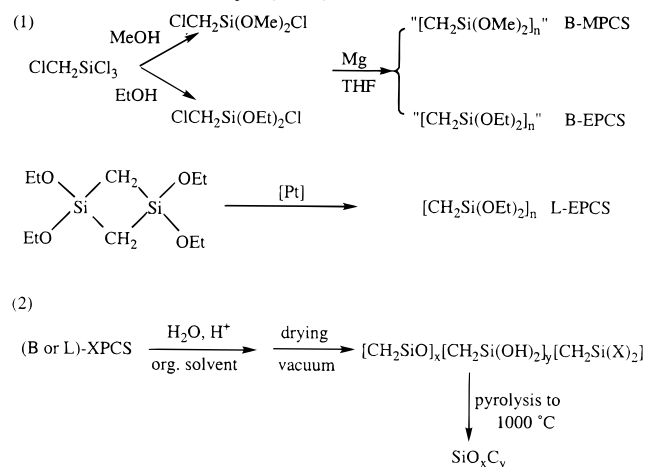
The polymer gels and the products obtained on pyrolysis at different temperatures were characterized by elemental analyses, FT-IR, solid-state NMR, TGA, and the BET test. The elemental analyses were performed by Galbraith Laboratories. IR spectra were obtained by using a Perkin-Elmer 1800 Fourier transform infrared spectrometer. The solid samples were first ground to a fine powder in air by using a mortar and pestle, followed by mixing with KBr, and then pressed into pellets for IR transmission studies. Solid-state NMR spectra were recorded on a Chemagnetics CMX-360 SSNMR spectrometer. The cross-polarization–magic-angle spinning technique (CP-MAS) was used to record the ¹³C NMR spectra, with a contact time of 3 ms, pulse delay of 3 s, and spinning speed of 4 kHz, and as well as for the ²⁹Si NMR spectra, with a contact time of 3 ms, pulse delay of 5 s, and spinning speed of 5 kHz. Single pulse with H decoupling experiments (1pda) were used for the ²⁹Si NMR spectra with pulse widths of 2 ms ($\theta = 30^\circ$), pulse delays of 60 s, and 1000 acquisitions. The peaks are labeled with the usual C, M_n , D_n , T_n , and Q_n notation.¹³ C, M, D, T, and Q respectively refer to $\text{SiC}_{4-x}\text{O}_x$ units with $x = 0, 1, 2, 3$, or 4, where n is the number of bridging O atoms surrounding Si. The combined rotation and multiple pulse spectroscopy (CRAMPS) of ¹H was run on a Chemagnetics CMX-360 SSNMR spectrometer with adipic acid as an external reference.

Thermogravimetric analyses (TGA) were recorded with a Netzsch instrument (model STA 409) equipped with an

- (8) Zhang, H.; Pantano, C. G. *J. Am. Ceram. Soc.* **1990**, *73*, 958.
 (9) Soraru, G. D.; Dallapiccola, E.; D'Andrea, G. *J. Am. Ceram. Soc.* **1996**, *79*, 2074.
 (10) Baney, R. H.; Eguchi, K.; Zank, G. A. *Soc. Chem. Jpn.* **1996**, *8*, 23.
 (11) Soraru, G. D.; Suttor, D. High-Temperature Stability of Sol-Gel-Derived SiO_xC_y Glasses. *J. Sol-Gel Sci. Technol.* In press.
 (12) Corriu, R. J. P.; Leclercq, D.; Mutin, P. H.; Vioux, A. *J. Mater. Sci.* **1995**, *30*, 2313.
 (13) Babonneau, F.; Bois, L.; Yang, C.-Y.; Interrante, L. V. *Chem. Mater.* **1994**, *6*, 51.
 (14) Soraru, G. D. *J. Sol-Gel Sci. Technol.* **1994**, *2*, 843.
 (15) Wilson, A. M.; Zank, G. A.; Eguchi, K.; Xing, W.; Yates, B.; Dahn, J. R. *Chem. Mater.* **1997**, *9*, 1601.
 (16) Babonneau, F.; Soraru, G. D.; D'Andrea, G.; Dirè, S.; Bois, L. *Mater. Res. Soc. Symp. Proc.* **1992**, *271*, 789.
 (17) Soraru, G. D.; D'Andrea, G.; Campostrini, R.; Babonneau, F.; Mariotto, G. *J. Am. Ceram. Soc.* **1995**, *78*, 379.
 (18) Liu, Q.; Apple, T.; Zheng, Z.; Interrante, L. V. *Mater. Res. Soc. Symp. Proc.* **1996**, *435*, 513.
 (19) Whitmarsh, C. K.; Interrante, L. V. *Organometallics* **1991**, *10*, 1336.
 (20) Rushkin, I. L.; Shen, Q.; Lehman, S. E.; Interrante, L. V. *Macromolecules* **1997**, *30*, 3141.

- (21) Shen, Q., Ph.D. Thesis, Rensselaer Polytechnic Institute, 1995.
 (22) Liu, Q.; Shi, W.; Babonneau, F.; Interrante, L. V. *Chem. Mater.* **1997**, *9*, 2434.

Scheme 1. Preparation of the Gels and Their SiO_xC_y Pyrolysis Products



alumina furnace. About 70 mg of the gel powders were loaded in alumina crucibles and heated at 5 °C/min up to 1550 °C in an argon (Ar) flow (100 mL/min). Samples for the surface area measurements were pyrolyzed in a silica tube furnace under Ar flow (100 mL/min) at 5 °C/min up to 600 and 1000 °C. When the set temperature was reached, the silica tube was taken out and air cooled to room temperature while the Ar flow was maintained over the sample. Isothermal treatments were also performed at 600 and 1000 °C for 1 and 4 h with the same heating/cooling schedule and in the same flowing Ar atmosphere. No apparent differences were observed for the samples obtained from these pyrolysis and thermal annealing experiments when N_2 was substituted for Ar or when Mo was used instead of alumina as the sample container.

Nitrogen adsorption-desorption isotherms were measured using a Carlo Erba (model Sorptomatic 1800) instrument. The powdered samples (ground in a mortar after pyrolysis) (300–500 mg) were degassed overnight at 40 °C (gel samples) or 150 °C (pyrolyzed gels). Nitrogen specific surface areas at 77 K were determined from a BET (Brunauer, Emmet, and Teller) analysis in the PP_0 range of 0.05–0.30 using a molecular cross sectional area of 0.163 nm² and a minimum of five data points. The pore size (radius) distribution was obtained from the desorption isotherm through the Barret, Joyner, and Halenda analysis.²³

Results and Discussion

The reactions involved in the synthesis of the hybrid carborosilane/siloxane gels derived from the polycarbosilanes and their pyrolytic conversion to SiO_xC_y are shown in Scheme 1 along with the designations employed for the three different sol-gel precursors. These three polycarbosilanes differ in terms of molecular structure and/or the nature of the alkoxy group, with the B-polycarbosilanes having a relatively low molecular weight [degree of polymerization (DP) = ca. 13; polydispersity (PD) = 1.5–1.8] and a hyperbranched²⁴ structure containing $[(\text{CH}_2)_3\text{Si}]$, $[(\text{CH}_2)_2\text{SiOR}]$, $[(\text{CH}_2)\text{Si}(\text{OR})_2]$, and terminal $[\text{Si}(\text{OR})_3]$ units in an approximate 2/8/20/11 ratio but with an "average" formula of $[\text{Si}(\text{OR})_2\text{CH}_2]$.²⁰ In contrast, the L-polycarbosilane has a higher molecular weight (DP = ca. 250) and a regular, linear structure with alternating Si and C atoms.²⁵

Characterization of the Hyperbranched Polymers. In general, the IR and SSNMR spectra obtained

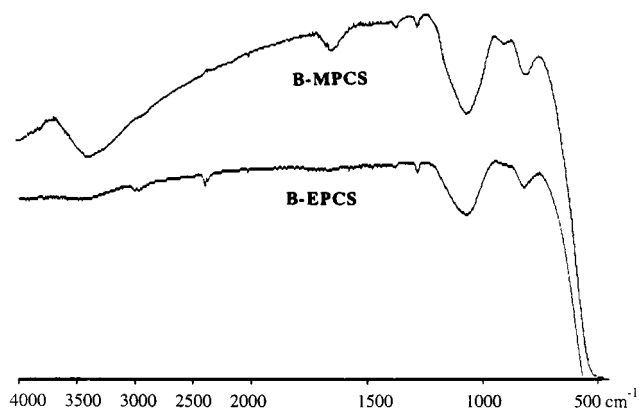


Figure 1. FTIR spectra of gels from B-MPCS/B-EPCS.

for the starting alkoxy polycarbosilanes and their sol-gel-derived products are similar to those previously reported for these materials.^{13,18,22} The FTIR spectrum of the B-EPCS polymer shows peaks attributable to the ethoxy groups bonded to silicon at 955, 1294, 1442, and 1482 cm⁻¹. All of the other observed peaks are consistent with the hyperbranched $-\text{SiCH}_2\text{Si}-$ backbone polymer structure.^{13,19,26} The ¹H NMR spectrum of this polymer consists of complex multiplets and broad peaks, also as expected on the basis of its hyperbranched structure.^{19,27} The multiplets at 0.2–1.0 ppm are attributed to the various SiCH_2Si and SiCH_3 groups. The peaks at 1.0–1.5 ppm are assigned to OCH_2CH_3 , whereas the peaks centered at 3.80 ppm are characteristic of OCH_2CH_3 . The ²⁹Si NMR spectrum shows four major groups of peaks. The peaks at around -46 ppm are attributable to the $\text{CH}_2\text{Si}(\text{OEt})_3$ groups (T units) with various environments. The peaks near -20 ppm can be assigned to various $(\text{CH}_2)_2\text{Si}(\text{OEt})_2$ groups (D units), whereas the $(\text{CH}_2)_3\text{Si}(\text{OEt})$ groups (M units) are believed to be responsible for the peaks near 2 ppm. The peaks at around -10 ppm are assigned to $(\text{CH}_2)_4\text{Si}$ groups (C units).²⁴ In the ¹³C NMR spectrum of this polymer, the ethoxy groups presumably give rise to the peaks near 20 and 60 ppm, while the carbons of the methylene units in various environments correspond to the peaks between -4 and 10 ppm.^{18,22,24}

The IR and NMR spectra of the methoxy polycarbosilane polymer (B-MPCS), which was synthesized by the same procedure, correspond closely to the results described above, except for the peaks associated with the alkoxy group.

Molecular Structure of the Dried Gels. The FTIR spectra of the gels from the two hyperbranched precursors (Figure 1) show the characteristic peaks due to the $\text{Si}-\text{O}-\text{Si}$ and $\text{Si}-\text{CH}_2-\text{Si}$ structures, which are quite similar to those found in the case of the gel derived from L-EPCS.^{18,22} But the gel from the methoxy polymer, B-MPCS, shows three more peaks at 900, 1631, and 3369 cm⁻¹, which could be attributed to a higher content of OH groups. This higher $\text{Si}-\text{OH}$ component is also evidenced in the ¹H CRAMPS NMR spectra of the gels. For the gel obtained from B-EPCS, the observed peaks and their assignments are 0.1 ppm (SiCH_2Si), 1.1 ppm (CH_3), 3.8 ppm (OCH_2CH_3), 6.7 ppm (spinning side-

(23) Gregg, S. J.; Sing, K. S. W. *Adsorption, Surface Area and Porosity*; Academic Press: London, 1982.

(24) 4. Frechet, J. M. J. *Science* **1994**, 263, 1710.

(25) Shen, Q.; Interrante, L. V. *Macromolecules* **1996**, 29, 5788.

(26) Shi, W., Ph.D. Thesis, Rensselaer Polytechnic Institute, 1995.

(27) Whitmarsh, C. K.; Interrante, L. V. *J. Organomet. Chem.* **1991**, 418, 69.

Table 1. Proportion of the Different Si Sites in the Various Gel Structures, as Derived from the ^{29}Si SSNMR Data

	L-EPCS ¹⁸	B-MPCS	B-EPCS
M %	0.75	18.9	12.3
C %			
(D ₁ +D ₂) %	94.8	45.9	48.0
(T ₂ +T ₃) %	4.48	35.2	39.7
Q %			
O/Si ratio	1.02	1.08	1.14
C-Si bond/Si	1.96	1.84	1.73

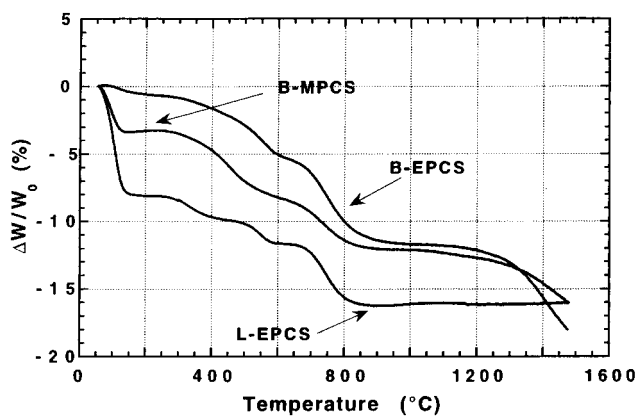
band). On the other hand, for the gel obtained from B-MPCS, the following peaks were found: 0–1.0 ppm ($\text{SiCH}_2\text{Si}/\text{CH}_3$), 3.3 ppm (OCH_3), 5.0 ppm (OH), 6.7 ppm (spinning sideband).

The ^{29}Si NMR spectra of the gels obtained from the hyperbranched polymers show three broad peaks at ~ 5 ppm (M units); ~ -20 ppm (D units); and ~ -60 ppm (T units). These peaks are shifted somewhat from the corresponding peaks in the hyperbranched alkoxy polycarbosilane precursors, and the weak peak corresponding to the M units is not seen in these spectra, presumably due to its overlap with the -20 ppm peak.

Actually, the peaks at -20 and -60 ppm can each be split into two components using deconvolution techniques. These two components correspond to the D₁ and D₂, T₂, and T₃ units arising from the presence of uncondensed species (OH or OR) bonded to Si. This was also evidenced in our studies of the L-EPCS gel system.¹⁸ The percentages of the different components that were obtained from the NMR data by using integration and deconvolution techniques are listed in Table 1. The results from the L-EPCS gel are also listed for comparison. From Table 1, we can see that the three systems have similar O/Si and C-Si bond/Si ratios at the gel stage due to the same average $\text{Si}(\text{OR})_2\text{CH}_2$ formula of the polymers, although the degrees of cross-linking are different. Also the gels from the two branched polymers have a similar distribution of Si sites, as expected for the similar hyperbranched structure of their precursors.

Appreciable differences are seen in the ^{13}C NMR spectra of the gels in which the gel obtained from B-MPCS has only one broad peak attributable to the methylene backbone, whereas the gel from B-EPCS has, in addition to the methylene backbone signal, two more peaks due to residual ethoxy groups. This could be attributed to the fact that methoxy silanes generally undergo hydrolysis more readily than their ethoxy analogues. Moreover, the increased steric hindrance associated with the hyperbranched polymer system may also contribute to incomplete hydrolysis and condensation. The combination of these factors is probably responsible for the higher OH content in the dried gel obtained from B-MPCS as well as the residual OEt groups (and OH) in the gel obtained from B-EPCS.

Conversion of the Dried Gels into SiO_xC_y Ceramics. The TGA curves obtained for the three gels are shown in Figure 2. A detailed study of the conversion mechanism from the hybrid polymer into silicon oxycarbide glass at 1000°C has already been reported for similar systems.^{18,22} For all of the gels, up to $\approx 600^\circ\text{C}$ the weight loss can be mainly assigned to the completion of condensation reactions which release water and alcohol, while the conversion from the polymeric network into an inorganic material occurs in the temper-

**Figure 2.** Thermogravimetric curves recorded for the three precursor gels.

ature range $600\text{--}900^\circ\text{C}$. By 1000°C the ceramic yield ranges from a value of 83% for the L-EPCS to 88% for the B-MPCS and B-EPCS samples. Above 1000°C , it is worth noting that the three samples show quite different thermal stabilities; indeed, the L-EPCS system is stable up to 1500°C , whereas the hyperbranched systems above $\approx 1200^\circ\text{C}$ undergo a decomposition process with a substantial weight loss of 3.6% and 6.3%, respectively.

The FTIR spectra of the samples obtained from the pyrolysis process are consistent with the structural evolution previously observed for the L-EPCS system,¹⁸ where the organic group content decreased and eventually disappeared on heating to 600°C and by 1000°C only the peaks corresponding to the inorganic Si-O-Si and Si-C-Si structures remain, evidencing the conversion from an organic/inorganic hybrid structure to a purely inorganic structure.

The ^{13}C NMR spectra of the pyrolyzed samples obtained from the B-EPCS gel are shown in Figure 3. The residual ethoxy peaks have disappeared by 600°C . At 1000°C , there is one very broad peak above 130 ppm and one peak centered at 13 ppm which can be assigned to free carbon and carbidic carbon, respectively. Again, these are similar to the changes observed for the L-EPCS system. For the B-MPCS system (Figure 4), at 1000°C the dominant signal is the free carbon peak and the peak due to carbidic carbon is very small. This suggests that the ceramic from the B-MPCS gel has a much higher free carbon content than the ceramic from the B-EPCS gel.

The ^{29}Si NMR spectra corresponding to the conversion process for the B-EPCS gel are shown in Figure 5. Comparing with the results obtained previously for the L-EPCS system, the B-EPCS system has a similar pattern and a full distribution of $\text{SiC}_{4-x}\text{O}_x$ sites at 1000°C due to the same redistribution mechanisms; however, the ^{29}Si NMR spectra of the B-MPCS system (Figure 6) show a significant shift of the distribution of Si sites toward the Q unit direction and it has a much higher Q unit content at 1000°C compared to both the L-EPCS and B-EPCS systems. The results of the integration and deconvolution of the spectra obtained for the ceramics at 1000°C are shown in Table 2. The elemental analysis results are shown in Table 3. The results obtained previously for the L-EPCS system are also listed for comparison.

The MAS NMR and chemical analysis results for the silicon oxycarbide glasses pyrolyzed at 1000°C are

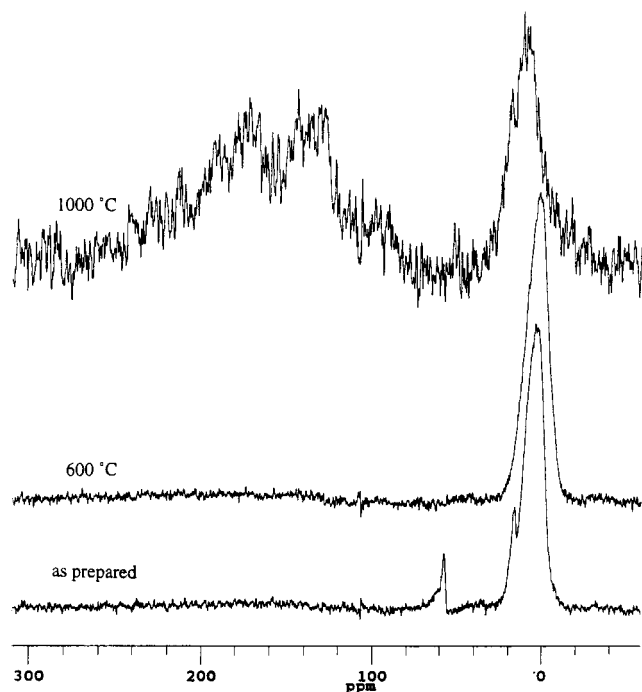


Figure 3. ^{13}C (CP-MAS) NMR spectra of the gel from B-EPCS and products after being pyrolyzed to different temperatures.

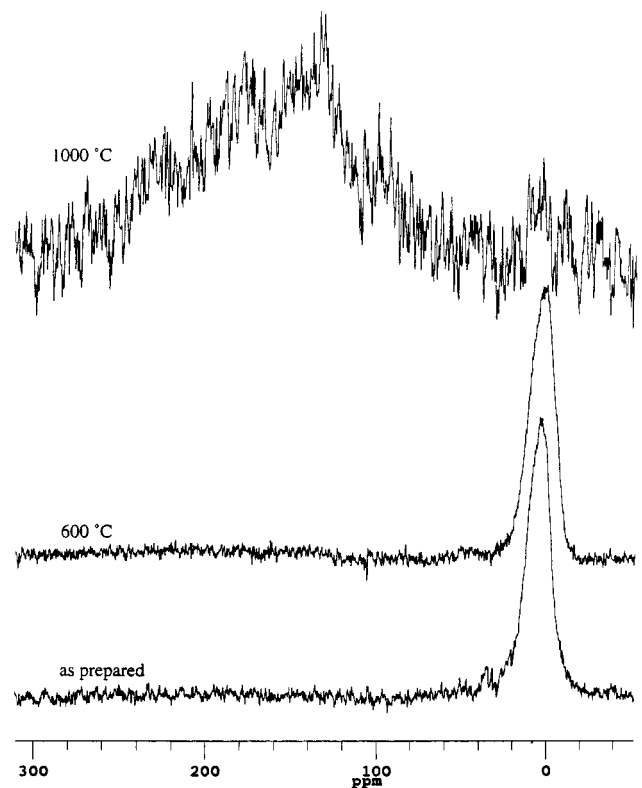


Figure 4. ^{13}C (CP-MAS) NMR spectra of the gel from B-MPCS and products after being pyrolyzed to different temperatures.

summarized in Table 4 in terms of the composition of the amorphous silicon oxycarbide network and the amount of free carbon, i.e., $\text{SiC}_x\text{O}_{2(1-x)} + y\text{C}_{\text{free}}$.

The SiO_xC_y ceramics obtained from B-EPCS and L-EPCS have relatively similar compositions, whereas that obtained from the B-MPCS is clearly quite different (Table 4). The latter has a higher O/Si ratio, free carbon content, and a very low C–Si bond/Si ratio (carbide

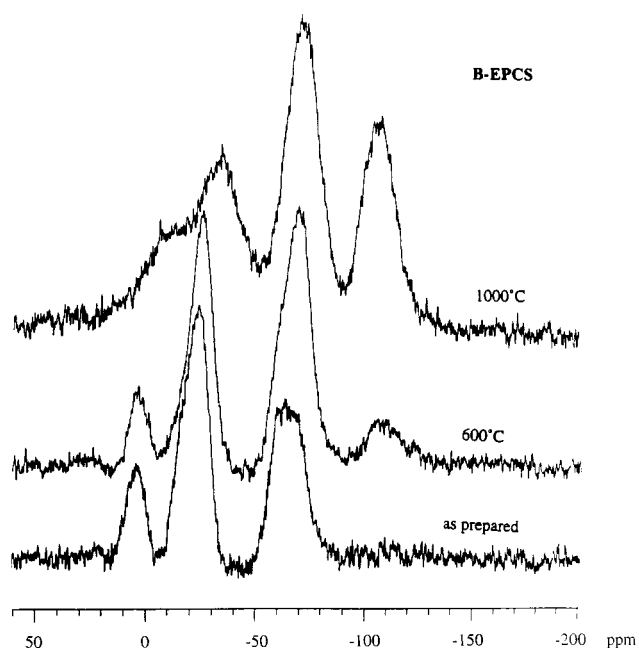


Figure 5. ^{29}Si (1pda-MAS) NMR spectra of the gel from B-EPCS and products after being pyrolyzed to different temperatures

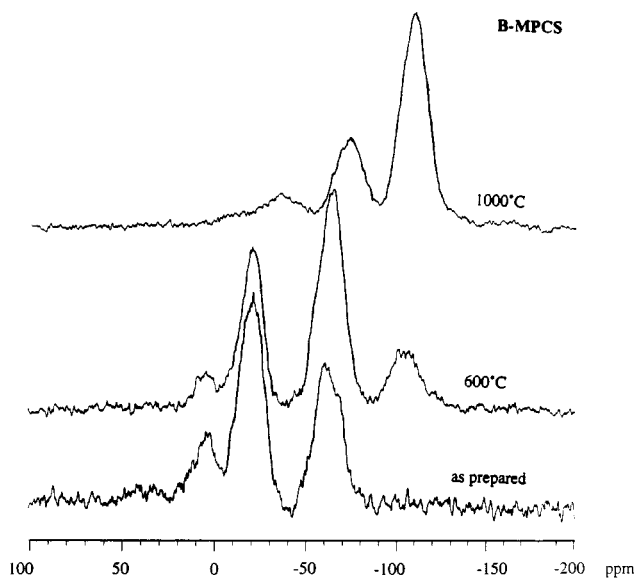


Figure 6. ^{29}Si (1pda-MAS) NMR spectra of the gel from B-MPCS and products after being pyrolyzed to different temperatures.

Table 2. Proportion of the Different Si Sites in the Various SiO_xC_y Ceramic (1000 °C) Structures, as Derived from the ^{29}Si SSNMR Data

	L-EPCS ¹⁸	B-MPCS	B-EPCS
M %	5.88		
C %	3.49		10.6
D %	36.6	14.0	29.6
T %	39.6	22.1	36.9
Q %	14.4	63.9	22.9
O/Si ratio	1.28	1.75	1.31
C–Si bond/Si	1.44	0.50	1.38

carbon content) in the ceramic compared to the other two ceramics. These differences are also evidenced by the high Q unit content in the ^{29}Si NMR spectrum and the large free carbon signal in the ^{13}C NMR spectrum at 1000 °C. On the basis of our previous findings,²² the

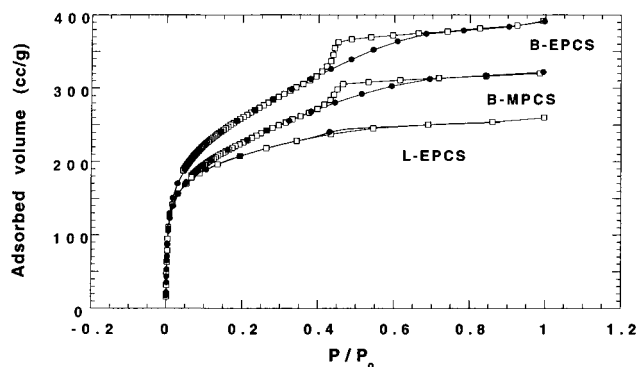


Figure 7. Nitrogen absorption (filled dots) and desorption (empty squares) isotherms of the studied gels.

Table 3. Elemental Analysis Results for the SiO_xC_y Ceramics (1000 °C) Obtained from the Three Different Gels

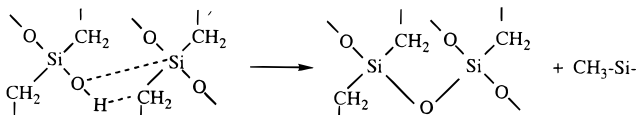
	Si, %	C, %	H, %	O, % ^a
L-EPCS ¹⁸	49.42	15.25	<i>b</i>	35.33
B-EPCS	45.39	14.34	0.74	39.53
B-MPCS	42.07	10.66	0.66	46.59

^a Calculated by difference. ^b H was not analyzed in this case.

Table 4. Compositional Formula Derived from the Elemental Analysis and ²⁹Si SSNMR Data for the SiO_xC_y Ceramics (1000 °C) Obtained from the Three Different Gels

L-EPCS	$\text{SiC}_{0.36}\text{O}_{1.28} + 0.33\text{C}_{\text{free}}$
B-MPCS	$\text{SiC}_{0.125}\text{O}_{1.75} + 0.465\text{C}_{\text{free}}$
B-EPCS	$\text{SiC}_{0.345}\text{O}_{1.31} + 0.392\text{C}_{\text{free}}$

Scheme 2. Si-OH-Induced Si-C Bond Cleavage in the Gel



higher content of OH groups in the B-MPCS gel is likely to facilitate the Si-C/Si-O bond rearrangement process, thereby resulting in a higher O/Si ratio after pyrolysis. As we have discussed previously,²² Si-OH-induced redistribution reactions (Scheme 2), involving the shift of H and the exchange of Si-O with Si-C bonds, facilitate Si-C/Si-O redistribution and lead to the loss of carbon from the SiO_xC_y network as either free carbon or volatile hydrocarbon products.

The Microstructure of the Gels and Their Ceramic Products. The absorption-desorption isotherms of the three gels as well as the pyrolyzed products show a BET type I behavior, suggesting that they are microporous solids (Figure 7).²³ The hysteresis loops are typical of “ink-bottle”-shaped pores. The pore size distributions of the precursor gels are reported in Figure 8. The three samples display enhanced probabilities of pores in the radius range of 16–21 Å. The B-EPCS gel shows a quite significant and narrow peak centered at ≈ 19 Å; the B-MPCS gel is characterized by a smaller and broader peak with a maximum still at ≈ 19 Å, whereas the L-EPCS sample shows a very small and broad peak with a maximum close to 18 Å.

In Table 5 are reported the BET surface area values obtained for the three gels and the corresponding pyrolyzed samples. The evolution of the surface area

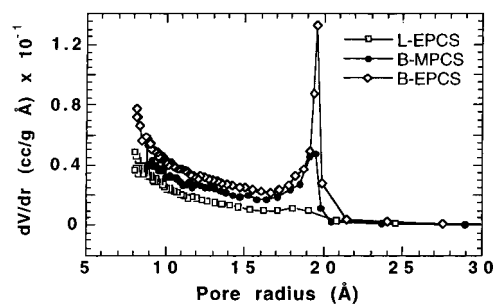


Figure 8. Pore size distribution for the precursor gels.

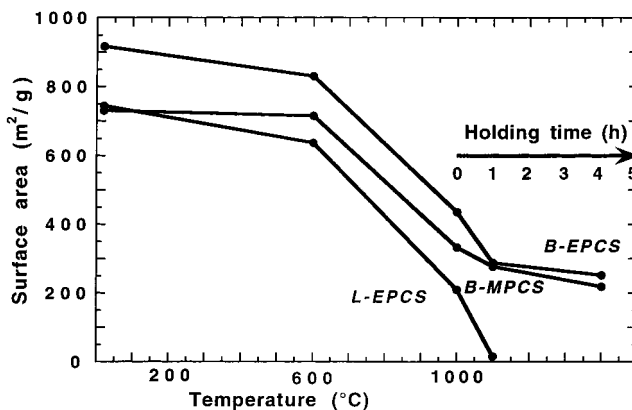


Figure 9. Evolution of the BET surface area with the pyrolysis temperature and holding time at 1000 °C.

Table 5. Surface Area of the Precursor Gels and Corresponding Silicon Oxycarbide Glasses

temp (°C)	surface area (m ² /g) (± 10)					
	L-EPCS gel		B-MPCS gel		B-EPCS gel	
	1 h	4 h	1 h	4 h	1 h	4 h
20	745		731		917	
600	637	556	715	688	830	782
1000	210	16	<10	333	277	218
						436
						280
						252

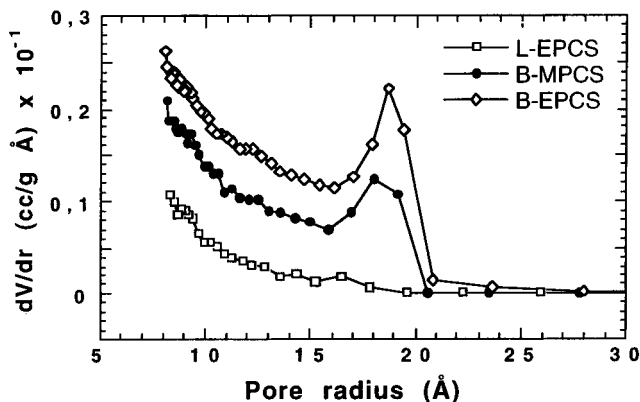


Figure 10. Pore size distribution for the silicon oxycarbide glasses pyrolyzed at 1000 °C.

with the pyrolysis temperature and with the holding time at 1000 °C is shown in Figure 9. All of the gels have high surface areas in the range 700–900 m²/g. Upon heating, the surface area remains almost unchanged up to 600 °C, but drops rapidly between 600 and 1000 °C. At 1000 °C the three samples still display high surface areas in the range of 200–436 m²/g and pore size (radius) distribution curves as shown in Figure 10. As can be observed in Figure 10, the samples obtained from the hyperbranched polymer still exhibit

an enhanced probability in the pore radius range of 16–21 Å with a maximum at ≈ 18 Å, whereas the corresponding peak is absent in the pore radius distribution curve of the ceramic derived from the L-EPSC system. Thus the pyrolysis treatment leads to a slight reduction of the pore radius (from ≈ 19 to ≈ 18 Å) for the hyperbranched system samples and to a complete closure (collapse) of the same (analogous) pore fraction in the silicon oxycarbide glass obtained from the linear gel precursor.

The isothermal treatment at 600 °C leads, after 4 h, to a slight decrease of the surface area that is more pronounced for the L-EPSC system ($\approx 20\%$) than for the branched system samples ($\approx 10\%$). The small decrease of the surface area observed for all the systems can be understood in the context of the lack of significant decomposition at this pyrolysis temperature. The main processes that occur in this temperature range are the continuous completion of condensation and rearrangement reactions.^{18,22} Therefore, the decrease in the surface area is probably caused by the closure of some pores due to the condensation and/or rearrangement of the network. These processes are the same for all three systems and this causes a parallel behavior for the three gels.

On the other hand, at 1000 °C the three samples display a quite different behavior, particularly after the isothermal holding. At this temperature, the isothermal treatment leads to a sharp drop in the surface area in the case of the L-EPSC system (with a BET value of 10 m²/g after 1 h at 1000 °C), whereas the porous microstructure of the oxycarbide glasses obtained from the two hyperbranched polycarbosilane gels seems more stable, and even after 4 h at 1000 °C, a relatively high surface area (≈ 220 – 250 m²/g) is still observed along with a distinct maximum in the pore radius distribution at ca. 18 Å.

These results appear to be related to the different microstructure of the preceramic network structures in these cases; in fact, compared to the gels obtained from the hyperbranched polycarbosilane, the L-EPSC preceramic gel has a higher probability of having very fine pores as well as a less distinct distribution at ≈ 18 Å. Therefore, it is much more inclined toward pore closure at high temperature than the other two gels. On the other hand, the hyperbranched systems essentially retain, even after 4 h at 1000 °C, the same pore radius distribution as the preceramic network. Similar surface area values (200–300 m²/g; measured after 2 h at 1000 °C) have been reported for SiO_xC_y glasses obtained by pyrolysis of polysiloxane gel precursors.^{6,28} However, in that case, the average pore radius was higher, i.e., ≥ 30 Å, and to our knowledge, this is the first time that very fine pores, radius ≈ 18 – 19 Å, have been observed to survive the pyrolysis treatment and lead to a microporous SiO_xC_y glass whose microstructure is stable for 4 h at 1000 °C. This effect is probably related to the slow sintering kinetics resulting from (i) the high viscosity of silicon oxycarbide glasses associated with the incorporation of tetravalent carbon atoms in the silica network and (ii) the presence of a secondary free carbon phase that can hinder the viscous deformation.

High-Temperature Stability of the SiO_xC_y Ceramics. Above 1300 °C Si–C–O glasses can undergo a

decomposition process with the evolution of SiO and CO and substantial weight loss. However, it is now well-recognized that the composition, and particularly the amount of excess carbon, can play an important role in controlling the high-temperature stability of silicon oxycarbide glasses both in oxidizing and in reducing atmospheres.^{10,11} In the case of the systems investigated here, however, the percentage of excess carbon, being similar for the three glasses, cannot account for their very different thermal stability behavior (see Figure 2). In particular, the L-EPSC and B-EPSC systems display a very close composition of the amorphous Si–C–O phase and the amount of free carbon (Table 4) but show quite different high temperature behavior. Therefore, we tentatively explain the different high-temperature evolution of our SiO_xC_y glasses in terms of their different microstructure.^{11,29} The thermal decomposition of SiO_xC_y ceramics involves the formation of volatile products such as CO and SiO that must be removed by diffusion from the system in order to allow the advancement of the reaction. Indeed, it is known that the thermomechanical degradation of the Si–C–O phase present in the commercially available Nicalon fibers shows a diffusion-controlled kinetics.³⁰ Accordingly, for the B-MPCS and B-EPSC samples pyrolyzed at 1000 °C, the diffusion of the reaction products from the bulk to the surface should be favored due to the formation of a stable microporous glass with pore size up to 18 Å. On the other hand, the L-EPSC precursor forms a SiO_xC_y glass with a compact microstructure at 1000 °C (surface area ≤ 10 m²/g after 1 h at 1000 °C) that could hinder the diffusion of the gaseous products to the surface, thereby limiting any further weight loss and resulting in a more thermally stable ceramic.

Conclusions

The pyrolysis of the B-MPCS, B-EPSC, and L-EPSC polycarbosilane/siloxane gels to SiO_xC_y ceramics follows a pattern similar to that found for other siloxane precursors. In particular, heating in the range from 100 to ca. 500–600 °C results mainly in a further condensation of the network structure which eliminates water and alcohol; above 600 °C this inorganic/organic hybrid network undergoes extensive Si–O/Si–C bond redistribution. This latter process results in some loss of volatile hydrocarbons but mainly leads to a combination of carbidic and free carbon whose relative proportion is controlled mainly by the O/Si and C/Si ratios in the starting gel system. In the case of gels which contain appreciable uncondensed Si–OH groups (in this case the gel obtained from the B-MPCS precursor), these Si–OH groups facilitate the Si–C/Si–O redistribution reactions; this results in a higher O/Si ratio in the oxycarbide glass with a corresponding decrease in the proportion of carbidic carbon and an increase in the free carbon content.

All the investigated gels and their pyrolyzed products exhibit relatively high surface areas and microporous

(28) Liu, C.; Chen, H. Z.; Komarneni, S.; Pantano, C. G. *J. Porous Mater.* **1996**, *2*, 245.

(29) Sorarù, G. D. The Role of Synthesis Conditions on the Microstructure and High-Temperature Stability of Gel-Derived Silicon Oxycarbide Glasses. Presented at the 99 Annual Meeting of the American Ceramic Society, Cincinnati, 1997.

(30) Labrugere, C.; Guette, A.; Naslain, R. *J. Europ. Ceram. Soc.* **1997**, *17*, 623.

structures. Moreover, their microporous structures can survive relatively high temperature (up to about 600 °C). However, it is apparent from the pore size distribution data (Figure 8) that these three gels have quite different microstructures and that these different microstructures lead to quite different SiO_xC_y ceramic products. The conclusion that these differences in microstructure are related more to the differences in the initial gel molecular or supramolecular structure than to the composition of the final SiO_xC_y ceramic is suggested by the fact that the ceramics obtained from the L-EPCS and B-EPCS precursors have quite similar chemical compositions, whereas the two ceramics which are most different in composition (those derived from B-EPCS and B-MPCS) are the most similar in terms of their porosity distribution and microstructural stability (see Table 4 and Figure 10).

During the pyrolysis the surface area of all the gels decreases because of the shrinking and/or collapse of the pores. In the case of the gels derived from the hyperbranched polycarbosilane precursors, the resulting silicon oxycarbide ceramics maintain relatively high surface areas, even at 1000 °C, with a distinct peak in the pore radius distribution at around 18–19 Å. However, these hyperbranched polycarbosilane-derived ceramics are apparently less stable toward weight loss at temperatures above 1000 °C than the corresponding

L-EPCS-derived SiO_xC_y , possibly owing to a denser microstructure in the latter case. These results show that the precursor architecture plays an important role in controlling the microstructure of the resulting silicon oxycarbide glass which, in turn, strongly affects its high-temperature stability.

The high ceramic yield, high surface area, porous structure, and microstructural stability of these gel systems make them of interest as precursors to SiO_xC_y ceramics, for potential use as catalyst supports or ceramic membranes for gas separation and, in the gel form, as interlayer dielectric materials (ILD) materials with low dielectric constants.

Acknowledgment. The work at the University of Trento was supported by MURST (40%). The work at RPI was supported by a grant from the Chemistry Division of the National Science Foundation, No. CHE-950930.

Supporting Information Available: FTIR spectrum, ^1H NMR spectrum, ^{29}Si NMR spectrum, and ^{13}C NMR spectrum of B-EPCS and ^1H CRAMPS NMR spectra, ^{29}Si (1pda-MAS) SSNMR spectra, and ^{13}C (CP-MAS) SSNMR spectra of the gels from B-MPCS/B-EPCS (7 pages). Ordering information is given on any current masthead page.

CM9804719